Low–Alloy Duplex, Directly–Quenched Transformation–Induced Plasticity Steel

H. L. Yi [a] J. H. Ryu [a] H. K. D. H. Bhadeshia [a,b] H. W. Yen [c] J. R. Yang [c]

[a] *Graduate Institute of Ferrous Technology, Pohang University of Science and Technology, Pohang 790-784, Republic of Korea*

[b] *Materials Science and Metallurgy, University of Cambridge, Cambridge CB2 3QZ, U.K.*

[c] *Department of Materials Science and Engineering, National Taiwan University, Taipei, Taiwan*

Abstract

A duplex microstructure consisting of allotriomorphic ferrite and austenite at ambient temperature, has been produced in a low–alloy steel, by a simple heat treatment which involves intercritical annealing followed by quenching. The tensile properties obtained are good, with a total elongation of some 28% at an ultimate tensile strength approaching 900 MPa. The form of the stress versus strain curve is suitable for automotive applications, but it is speculated that the steel could be better exploited in a hot–pressed form.

Key words: Duplex steel, Low alloy, Quenched, Hot–press forming

TRIP–assisted steels contain retained austenite, which is stabilised, not by the use of expensive solutes, but by the partitioning of carbon into the residual austenite during the course of the bainite reaction. The final microstructure contains allotriomorphic ferrite as the dominant phase, and a mixture of carbide–free bainitic ferrite and carbon–enriched austenite; some martensite may also be present. The bainite is produced by incorporating a step in the production process whereby the steel is held approximately isothermally below the bainite–start temperature of the austenite.

The major phase in TRIP–assisted steels is the allotriomorphic ferrite ($\approx 70\%$) which in itself leads to an enhancement of the carbon concentration of the re-

Email addresses: hityihl@postech.ac.kr (H. L. Yi), hkdb@cam.ac.uk, corresponding author (H. K. D. H. Bhadeshia).

maining austenite; and the purpose of the bainite reaction is primarily to induce further partitioning of carbon into the residual austenite [1, 2]. Suppose now that the fraction of ferrite can be increased to such an extent that the austenite becomes sufficiently enriched to remain stable at ambient temperature, then it would no longer be necessary to include the step associated with the formation of bainite. The steel could then simply be quenched to retain the mixture of allotriomorphic ferrite and untransformed austenite.

Recent work [3, 4] suggests that the required levels of allotriomorphic ferrite might be obtained using steels containing sufficient aluminium, which has been known for some time to promote ferrite [5]. The purpose of the work presented here, was therefore, to explore this concept and investigate the properties associated with the duplex, low–alloy $\alpha + \gamma$ microstructure.

The alloys were manufactured as 34 kg ingots of $100 \times 170 \times 230$ mm dimensions using a vacuum furnace. The actual composition is:

Fe-0.4C-0.22Si-1.03Mn-2.95Al wt%

The choice of this particular combination of alloying elements is based on previous experience on the design of δ–TRIP steels [4] where the microstructure was akin to conventional TRIP–assisted steels. Since this work has been published in depth, we shall avoid repeating the design procedures, suffice it to say that the aluminium is critical in ensuring sufficient allotriomorphic ferrite, and hence the right level of carbon in the remaining austenite. The main achievement in the present work is not the alloy design but rather the heat treatment.

The ingot was reheated to 1200°C for rough rolling to make 25–30 mm slabs followed by air cooling. These slabs were then reheated to 1200°C and hot–rolled to 3 mm in thickness; 1.2 mm thick sheets were then produced by cold rolling. It is possible that the high aluminium concentration means that some of the hot–rolling is conducted in the two–phase $\alpha + \gamma$ field, but it has been shown that this is feasible because of the high temperatures at which the ferrite is stable [4]. The heat treatments were conducted using $1.2 \times 4 \times 11$ mm cold rolled sheets in a CCT–AY (ULVAC-RIKO) simulator where the samples are heated at $20^{\circ}\mathrm{C\,s^{-1}}$ to 800, 850, 900, 950 °C and soaked for 3 min in a nitrogen atmosphere to allow some austenite to form, respectively, followed by quenching at $80^{\circ}\mathrm{C\,s^{-1}}$ to ambient temperature. Samples for tensile tests were machined from these blanks to ASTM standard E8M-00 with elongation measured on a 10 mm gauge length following tension at $3.3 \times 10^{-3}\,\mathrm{s^{-1}}$.

Microscopy samples were prepared using standard methods and etched in 2 wt% nital. High resolution observations were done using a field–emission scanning electron microscope operating at 10 kV accelerating voltage. X-ray diffraction was performed on specimens polished using 4000 grit sand paper

and chemically polished using 2 wt% nital. The diffraction covered 2θ from $35 - 106^\circ$ with a 3 s and 9 s step of 0.02° for 10×10 mm of undeformed zone and 10×4 mm of near fracture zone, respectively, using $Cu_{K\alpha}$ radiation. Reitveld analysis and cell refinement were used to calculate the retained austenite content; these procedures were implemented using the TOPAS 3.1 software. The thin foils for investigation by transmission electron microscopy were produced by punching discs from steel sheets which were pre–thinned mechanically to 100 μm, and and then twin–jet electropolished to perforation using a mixture of 5 % perchloric acid, 20 % glycerol, and 75 % ethanol (in vol%) at 10°C at a potential of 35 V. They were examined on an FEI Tecnai G2 F20 field emission gun transmission electron microscope.

Equilibrium phase stability calculations conducted using MTDATA [6] with the TCFE5 database are illustrated in Fig. 1, where the carbon concentration and phase quantities are plotted as a function of the aluminium concentration while keeping the contents of the other solutes fixed. The calculations were done initially allowing the existence of ferrite, austenite and cementite; however, cementite does not in fact form in practice and hence the diagrams presented in Fig. 1 are calculated on the basis of just ferrite and austenite – it would be wise in future work to examine the period required at the intercritical annealing temperature for cementite to appear. It is clear from these calculations that the experimental alloy can indeed be intercritically annealed such that the residual austenite at the annealing temperature ends up with carbon concentrations comparable to those found in the retained austenite of ordinary TRIP–assisted steels [7, 8].

To check these estimates, the alloy was intercritically annealed at a variety of temperatures and followed by quenching in a thermomechanical simulator for sheet steel [4]. The results are compared against the equilibrium calculations in (Table 1), where the fraction of austenite is that which exists at the intercritical annealing temperature. The experimental data therefore represent the fraction of austenite including those regions which transformed into martensite. The calculations underestimate the amount of austenite, presumably because the time at the intercritical annealing temperature was only 3 min, which is not sufficient to allow the equilibrium fraction of ferrite to form.

Scanning electron micrographs of the simple structures obtained are illustrated in Fig. 2a, for four different intercritical annealing treatments. Table 1 shows the measured fraction of residual austenite (V_γ^{IC}) at the intercritical annealing temperature and that retained (V_γ^r) at ambient temperature following quenching. The latter quantity was measured using X–ray diffraction and Reitveld analysis as described earlier. There is almost no martensite present in the microstructure generated by intercritical annealing at 800°C, which is expected given that the M_S temperature of the residual austenite as listed in Table 1 is only 78°C, which may be an overestimate since the equation used [9] does not

take into account the grain size of the austenite. The scale of the austenite regions, at about $4\,\mu$m (Fig. 2) is in the domain where a 40°C suppression is expected when compared with a grain size an order of magnitude larger at $40\,\mu$m [10].

Given the small amount of martensite assessed to be present in the 800°C annealed sample, it was selected for detailed transmission electron microscopy in the condition prior to tensile testing. Fig. 3 shows a significant region of austenite which contains a small amount of α'–martensite identified using the morphological observation of plates, electron diffraction and the fact that the orientation relationship is close to what is expected. It is interesting that the plates do not grow right across the austenite region but seem to terminate before impingement, indicating that the driving force for transformation is small [11]. Most islands of austenite did not contain martensite; supporting transmission microscopy evidence is excluded for brevity but will be made available on the world wide web. This is to be expected given that the carbon concentrations of the austenite, and their individual sizes, are unlikely to be identical, as shown recently [12].

Fig. 4 summarises the results from tensile tests. It is evident that the greatest ductility is obtained in the samples intercritically annealed at the lowest temperatures, whereby the amount of martensite is minimised and the carbon concentration of the retained austenite is maximised. X–ray measurements of the austenite content following tensile testing, in the necked region of the broken samples confirmed that the retained austenite decreased in all cases to a value of about $V_\gamma^r \approx 0.05 \pm 0.01$. This shows that the austenite exhibits a TRIP effect; although the contribution of this transformation plasticity *per se* to the overall behaviour cannot be assumed [13] from these tests, it is evident that the tensile curves show significant work–hardening during the course of deformation. At the very least, the formation of martensite during the deformation contributes to the composite effect that leads to greater resistance to plastic instability [14, 15].

The steel developed evidently has respectable properties when intercritically annealed under appropriate conditions. The fact that the duplex structure can be produced by direct quenching suggests another scenario of applications. The forming of strong steels is technologically challenging because of the effects of springback [16]. In the case of TRIP–assisted steels, the decomposition of retained austenite during the forming process itself, limits its exploitation in the context of energy absorption during subsequent service deformation, for example in a crash. We suggest that the present steel can in principle be hot–press formed [17, 18] at 800°C followed by die–quenching, and furthermore, would retain its duplex microstructure unaffected by deformation, into the final component. Thus, although the strength obtained does not compete against conventional hot–press forming steels [19–21], there are not

only significant engineering and metallurgical advantages, but also potential cost savings if the cold forming operation is more expensive. Fig. 4c shows that the properties of the present alloy in terms of elongation in particular are superior to hot–press formed martensitic steels at a lower ultimate tensile strength.

It has been shown possible to design a low–alloy steel which on intercritical annealing at 800°C leads after quenching, to a duplex microstructure which is predominantly a mixture of ferrite and retained austenite. The process is made possible partly but the addition of aluminium which permits a large fraction of ferrite to be introduced at a high temperature. The mechanical properties obtained are promising in terms of strength and elongation, and suggest a possible application in the context of hot–press formed components.

We are grateful to Professor Nackjoon Kim for laboratory facilities at GIFT, and to POSCO for the Steel Innovation Programme. Support from the World Class University Programme of the National Research Foundation of Korea, Ministry of Education, Science and Technology, project number R32–2008–000–10147–0 is gratefully acknowledged.

References

[1] O. Matsumura, Y. Sakuma, H. Takechi: Transactions of the Iron and Steel Institute of Japan 27 (1987) 570–579.
[2] O. Matsumura, Y. Sakuma, H. Takechi: Scripta Metallurgica 27 (1987) 1301–1306.
[3] S. Chatterjee, M. Murugananth, H. K. D. H. Bhadeshia: Materials Science and Technology 23 (2007) 819–827.
[4] H. L. Yi, K. Y. Lee, H. K. D. H. Bhadeshia: Proceedings of the Royal Society A 467 (2010) 234–243.
[5] H. I. Aaronson, H. A. Domian, G. M. Pound: TMS–AIME 236 (1966) 781–796.
[6] NPL: MTDATA: Software, National Physical Laboratory, Teddington, U.K. (2006).
[7] H. K. D. H. Bhadeshia: Bainite in Steels, 2nd edition: Institute of Materials, London, 2001.
[8] B. DeCooman: Current Opinion in Solid State and Materials Science 8 (2004) 285–303.
[9] B. Mintz: The influence of aluminium on the strength and impact properties of steel: in: B. C. de Cooman (Ed.), TRIP–Aided High Strength Ferrous Alloys: University of Ghent, Belgium, 2002: pp. 379–382.
[10] H. S. Yang, H. K. D. H. Bhadeshia: Scripta Materialia 60 (2009) 493–495.
[11] S. Chatterjee, H. S. Wang, J. R. Yang, H. K. D. H. Bhadeshia: Materials Science and Technology 22 (2006) 641–644.

[12] E. Jimenez-Meiero, N. H. van Dijk, L. Zhao, J. Sietsma, S. E. Offerman, J. P. Wright, S. van der Zwaag: Acta Materialia 55 (2007) 6713–6723.
[13] H. K. D. H. Bhadeshia: ISIJ International 42 (2002) 1059–1060.
[14] Y. Tomota, K. Kuroki, T. Mori, I. Tamura: Materials Science and Engineering 24 (1976) 85–94.
[15] H. K. D. H. Bhadeshia, D. V. Edmonds: Metal Science 14 (1980) 41–49.
[16] N. Kuhn: Journal of the Australian Institute of Metals 12 (1967) 71–76.
[17] Norrbottens Jaernverk A. B.: Manufacturing of a hardened steel article: Patent gb1490535: Norrbottens Järnverk AB: Sweden (1977).
[18] G. Berglund: The history of hardening of boron steel in Northern Sweden: in: M. O. K. Steinhoff, B. Prakash (Eds.), 1st International Conference on Hot sheet metal forming of high–performance steel, CHS2: GRIPS media GmbH, Kassel, Germany, October 22–24, 2008: pp. 175–177.
[19] D. W. Fan, H. S. Kim, B. C. D. Cooman: Steel Research International 80 (2009) 241–248.
[20] M. Suehiro, J. Maki, K. Kusumi, M. Ohgami, T. Miyakoshi: Properties of aluminium–coated steels for hot–forming: Tech. Rep. 88: 16–21: Nippon Steel Corporation Technical Report (2003).
[21] M. Naderi: Hot stamping of ultra–high strength steels: Ph.D. thesis: RWTH Aachen: Germany (2007).
[22] H. L. Yi, S. Ghosh, H. K. D. H. Bhadeshia: Materials Science & Engineering A 527 (2010) 4870–4874.

Table 1
Comparison of calculated equilibrium quantities with measured values. T_{IC} represents the intercritical annealing temperature, V_γ^{IC} the fraction of residual austenite at that temperature (measured using quantitative metallography as described in [22]), V_γ^r is the fraction of austenite retained at room temperature, and M_S is the calculated martensite–start temperature of that austenite. This last calculation is due to [9]. C_γ is the carbon concentration of the austenite.

Calculated for equilibrium			Calculated	Measured	Measured
T_{IC} / °C	V_γ^{IC}	C_γ/ wt%	M_S / °C	V_γ^{IC}	V_γ^r
800	0.26	1.22	78	0.28±0.03	0.24 ± 0.01
850	0.28	1.08	138	0.35±0.04	0.14 ± 0.01
900	0.30	0.98	180	0.38±0.01	0.13 ± 0.01
950	0.31	0.90	214	0.46±0.01	0.12 ± 0.01

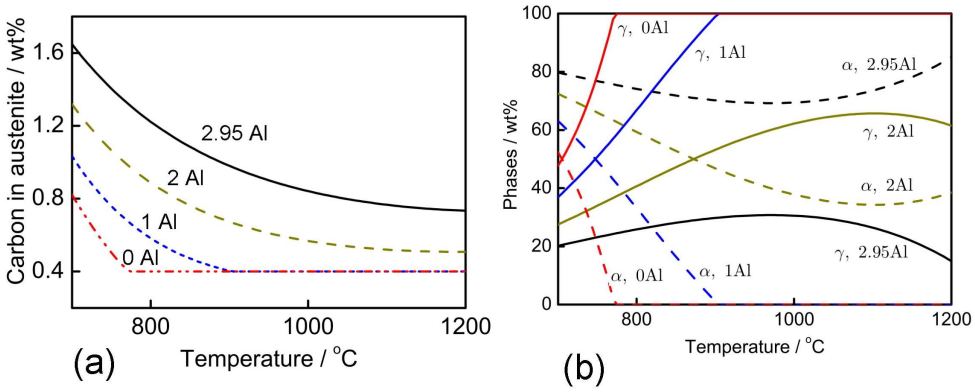

Fig. 1. Effect of aluminium addition on the (a) carbon concentration and (b) percentage of austenite in equilibrium.

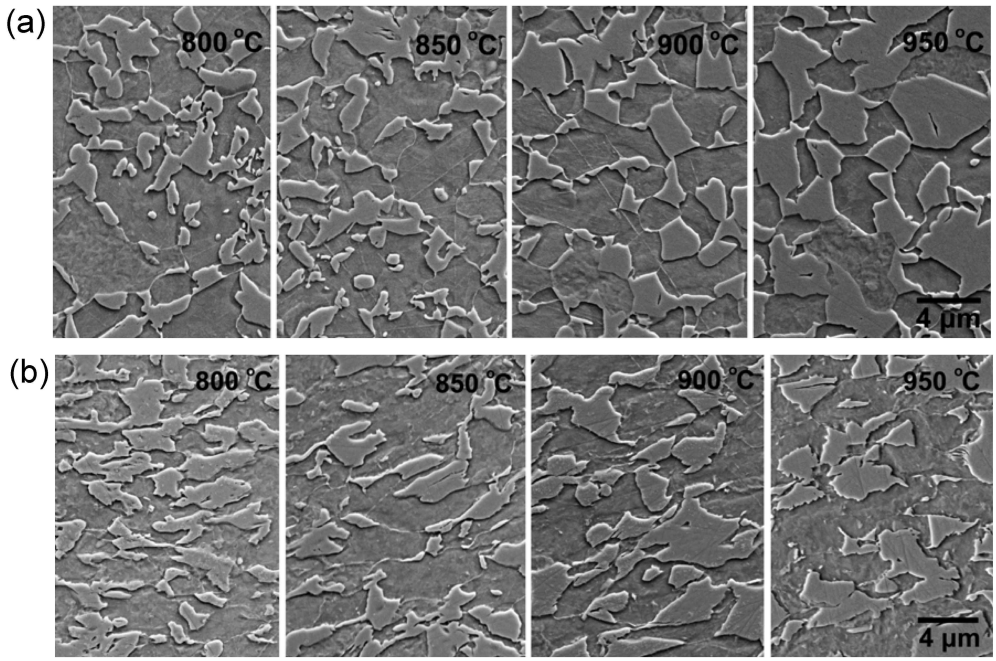

Fig. 2. Scan electronic microscopy reveals pre-austenite and allotriomorphic ferrite, (a) before deformation, (b) near fracture after tensile test.

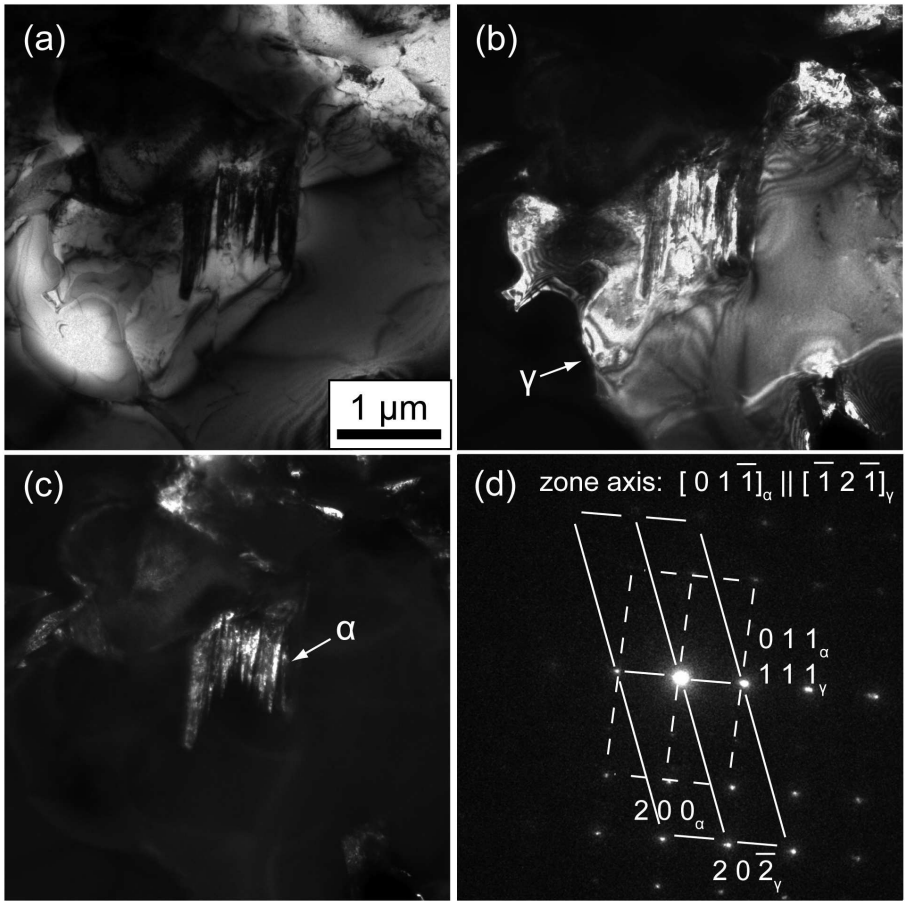

Fig. 3. Transmission micrographs of 800 °C samples. (a) Bright field image of α') in austenite. (b) Corresponding dark field image using $(\overline{2}02)_\gamma$ diffraction spot. (c) Corresponding dark field image using $(\overline{2}00)_{\alpha'}$. (d)Corresponding diffraction pattern of the α'/γ orientation relationship which can be approximated to be that by Nishiyama–Wassermann.

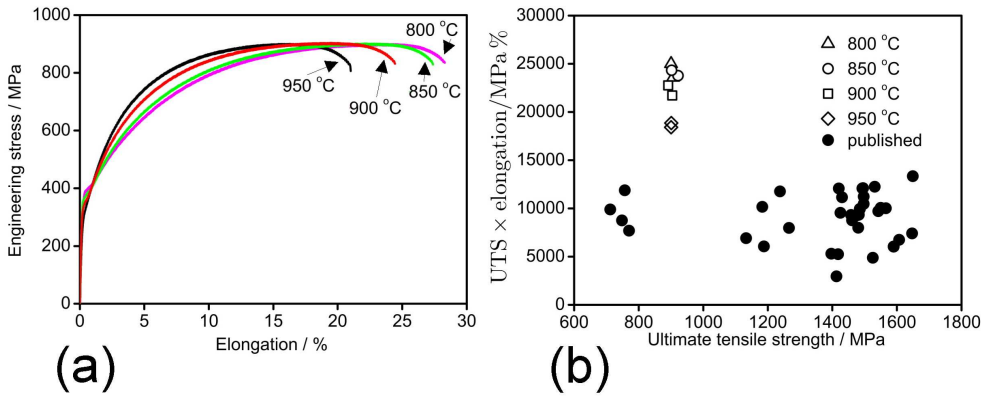

Fig. 4. (a) Tensile behaviour as a function of the intercritical annealing temperature. (b) The product of ultimate strength and elongation, an admittedly crude measure of formability, as a function of tensile strength. The published data are from [19–21].